Competitive Diels–Alder and ene addition of *N*-arylmaleimides to 7-dehydrocholesteryl acetate

WILLIAM J. LEIGH,[1] DONALD W. HUGHES, AND D. SCOTT MITCHELL[2]
Department of Chemistry, McMaster University, Hamilton, Ont., Canada L8S 4M1

Received April 21, 1992

WILLIAM J. LEIGH, DONALD W. HUGHES, and D. SCOTT MITCHELL. Can. J. Chem. **70**, 2730 (1992).

Thermolysis of *N*-phenyl, *N-para*-biphenyl, and *N-para,para'*-terphenylmaleimide with 7-dehydrocholesteryl acetate in benzene solution at 200°C yields mixtures of four cycloadducts in relative yields that are essentially independent of the maleimide substituent. The three major products are those of ene addition to C_7 of the steroid with abstraction of the proton at C_9 or C_{14}. The α-*endo*-Diels–Alder adduct is formed as a minor product. The structures of the adducts have been elucidated on the basis of one- and two-dimensional ^1H and ^{13}C NMR spectroscopic techniques, including homonuclear ^1H decoupling, NOE, ^1H–^1H COSY, heteronuclear ^1H–^{13}C shift correlation, and TOCSY 2-D experiments, and the results of molecular mechanics (MMX) calculations. The combination of these techniques has made it possible to almost completely assign the ^1H and ^{13}C NMR spectra for two of the ene adducts and the Diels–Alder adduct from reaction of 7-dehydrocholesteryl acetate with *N*-phenyl maleimide.

WILLIAM J. LEIGH, DONALD W. HUGHES et D. SCOTT MITCHELL. Can. J. Chem. **70**, 2730 (1992).

La thermolyse des *N*-phényl, *N-para*-biphényl et *N-para,para'*-terphénylmaléimides en présence d'acétate du 7-déhydrocholestéryle, en solution dans le benzène, à 200°C, fournit des mélanges de quatre cycloadduits dont les rendements relatifs sont essentiellement indépendants du substituant de la maléimide. Les trois produits principaux correspondent à une addition ène sur la position C_7 du stéroïde, accompagnée d'un enlèvement de proton en C_9 ou en C_{14}. L'adduit de Diels–Alder α-*endo* se forme comme produit mineur. On a déterminé les structures à l'aide de techniques de RMN du ^1H et du ^{13}C, uni- et bidimensionnelles, comprenant des expériences de découplage homonucléaire du ^1H, d'eOn, de COSY ^1H–^1H, de corrélation hétéronucléaire de déplacements ^1H–^{13}C et des expériences TOCSY en 2-D, et de résultats de calculs de mécanique moléculaire (MMX). Grâce à l'ensemble de ces techniques, il a été possible d'attribuer pratiquement tous les spectres RMN du ^1H et du ^{13}C de deux des adduits ène et de l'adduit de Diels–Alder obtenus par la réaction de l'acétate du 7-déhydrocholestéryle avec la *N*-phénylmaléimide.

[Traduit par la rédaction]

Introduction

The reactions of steroidal dienes such as 7-dehydrocholesterol (**1**) and ergosterol (**2**) with common dienophiles have been studied in some detail (1–13). Acyclic dienophiles such as dialkyl azocarboxylates (1–3), dimethyl acetylenedicarboxylate (4), acrylonitrile (5), and carbonyl dicyanide (6) have been reported to undergo ene addition with **1** (1–5), **2** (6), and the corresponding acetate esters to the complete exclusion of Diels–Alder cycloaddition. Evidently, Diels–Alder addition is preferred only with particularly powerful dienophiles such as *N*-phenyltriazolinedione (7, 8), 1,4-phthalazinedione (9), or singlet oxygen (10), or with acyclic alkenes when the steroidal diene moiety is part of a higher conjugated system (11).

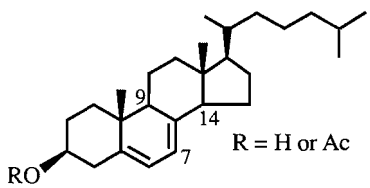

1

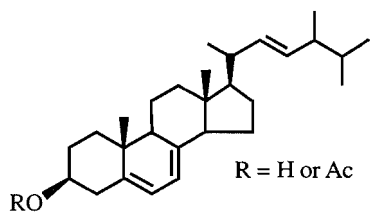

2

The reaction of maleic anhydride with ergosteryl acetate, which was first investigated almost 60 years ago (12), has been the subject of some confusion over the years (12–14). The reaction is now known to yield a mixture of the ene and Diels–Alder adducts shown in eq. [1] (14). The structures of the four products (**3–5**) have been assigned on the basis of derivativization studies and ^1H NMR spectroscopy (14), following the pioneering studies of Huisman and co-workers on the reactions of dienophiles with 7-dehydrocholesteryl acetate (**1**) (1, 3).

As part of our continuing studies of the effects of thermotropic liquid crystals on the reactivity of guest molecules (15), we have investigated the reaction of **1** with a series of *N*-aryl maleimides (**6–8**). A preliminary account of the reaction of **7** with **1** in isotropic and steroidal liquid crystalline solvents has been published (16). As is the case with maleic anhydride and **2**, a mixture of Diels–Alder and ene adducts are obtained as the major products from this reaction (eq. [2]). The three ene adducts were originally identified on the basis of diagnostic similarities between their ^1H NMR spectra and those of the ene adducts of **1** with acyclic dienophiles (1, 3).

[1]Natural Sciences and Engineering Research Council of Canada University Research Fellow, 1983–1993. Author to whom correspondence may be addressed.

[2]Present address: Uniroyal Chemical Limited, Guelph, Ont.

[1]

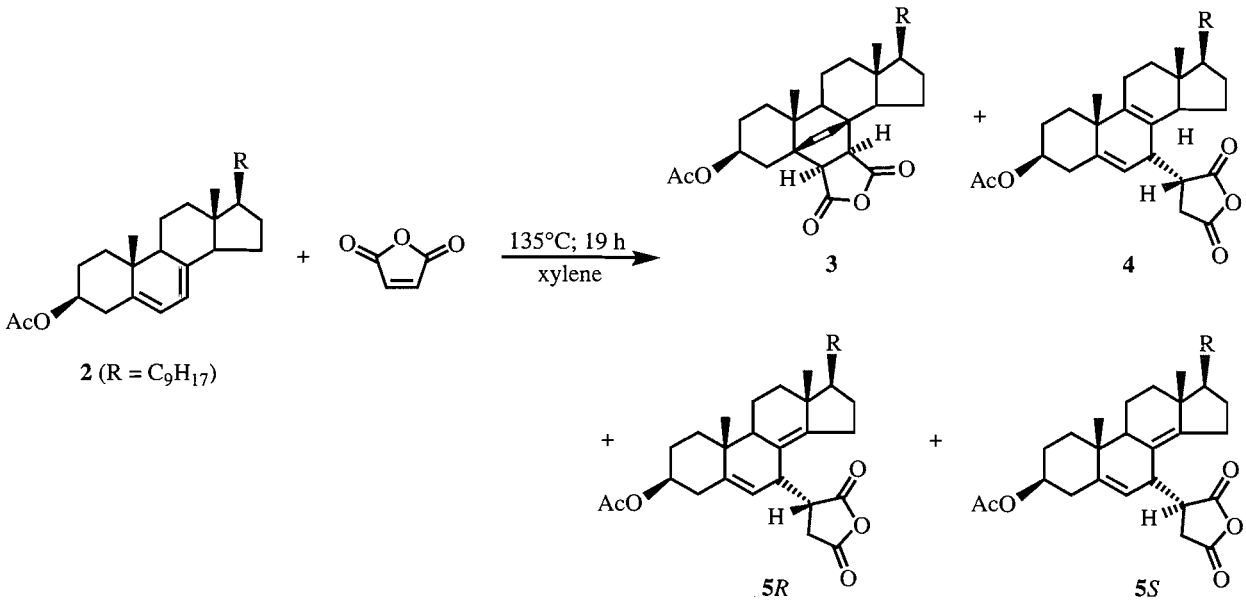

2 (R = C_9H_{17})

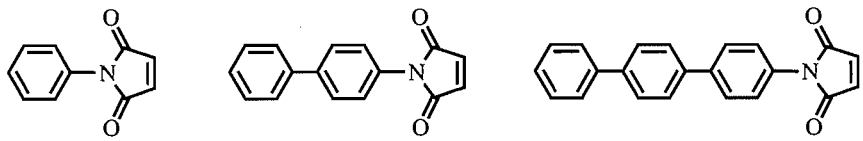

6 7 8

[2]

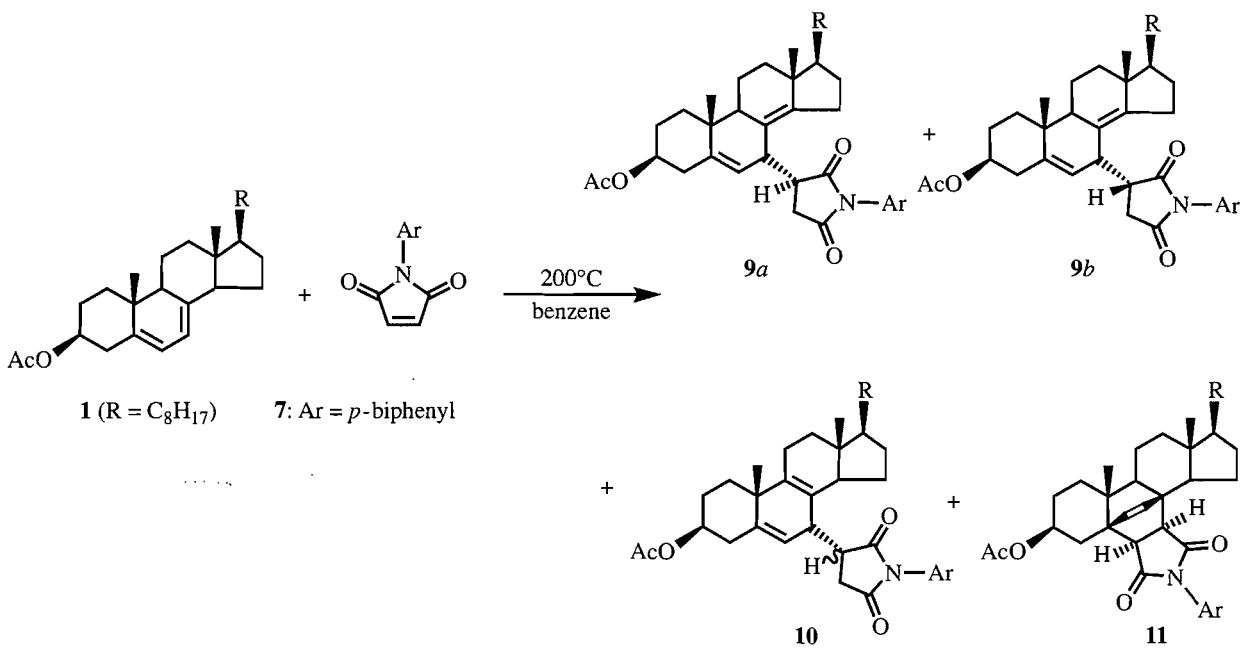

1 (R = C_8H_{17}) 7: Ar = *p*-biphenyl

In this paper, we report the results of a study of the reaction of **6–8** with **1** in benzene solution. We were particularly interested in rigorously verifying our structural assignments for **9** and **10**, which were made on the basis of ^{1}H chemical shift arguments following the rationale developed by Huisman and co-workers in identifying the ene adducts of **1** with dimethyl acetylenedicarboxylate (**12**) (eq. [3]) (4). The chemical shifts of the 18- and 19-methyl protons are very different in the ^{1}H NMR spectra of **13** and **14**. From examination of molecular models, Huisman and co-workers reasoned that the geometry of 18-CH_3 in relation to the C_8—C_9 double bond in **14** should result in its protons experiencing greater shielding than the corresponding ones in **13**. The methyl-proton regions of the ^{1}H NMR spectra of **9***a*,*b* and **10** (Ar = *para*-biphenyl) bear marked similarities to those of **13** and **14**, and our initial structural assignments were made on this basis. This same rationale has been used by numerous other workers in assigning the

[3]

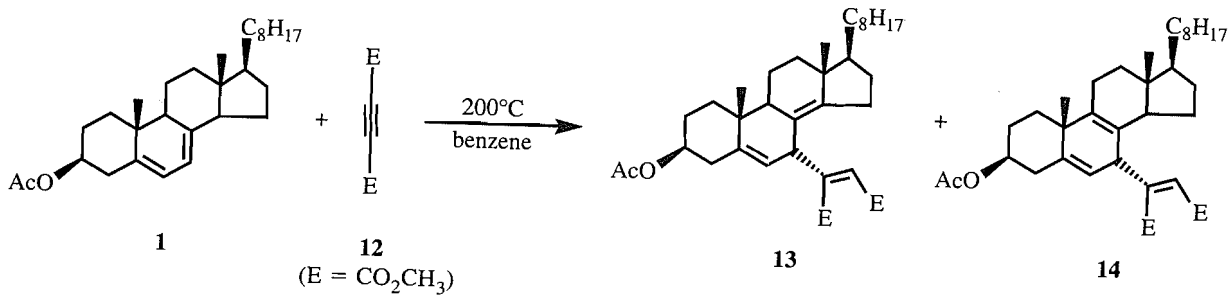

1 12 ($E = CO_2CH_3$) 13 14

structures of the products of ene additions to steroidal dienes (1–3, 5, 6, 14), but has evidently never been verified using modern NMR techniques.

In the present work, we attempted to verify our initial assignments using a more rigorous spectroscopic approach. We carried out various two-dimensional chemical shift correlation experiments, in order to assign the individual resonances in the rather complex ^1H and ^{13}C NMR spectra of these molecules. For three of the adducts, we also carried out homonuclear proton decoupling, NOE, and TOCSY 2-D experiments to help identify individual protons whose assignments on the basis of the other 2-D experiments are inconclusive. Molecular mechanics (MMX) calculations were also carried out in order to assist in our assignments in some cases. In particular, we wondered if it might be possible to conclusively identify the differences in the structures of the B and C rings in the two adduct types, through complete assignment of the B-, C-, and D-ring carbon and proton resonances. As shown in the partial structures below, differentiation of the two adduct structures is possible if the protons at C-11, C-12, C-15, and C-9/14 can be rigorously identified. We also employed these methods to establish the stereochemistry in the Diels–Alder adduct **11**, in order to verify the assignment made by Jones *et al.* for the Diels–Alder adduct (**3**) obtained from the reaction of ergosteryl acetate (**2**) with maleic anhydride (14).

The reaction of **1** and **6–8** in liquid crystalline solvents, which was the reason for our initial interest in this system, is described in a separate publication (17).

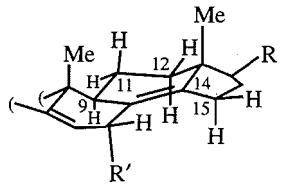

9

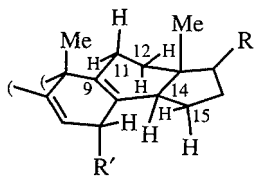

10

Results and discussion

N-Biphenyl- and *N*-terphenylmaleimide (**7** and **8**, respectively) were synthesized by condensation of the appropriate aromatic amine with maleic anhydride, following the method of Crivello (18).

Reaction of **6–8** with equimolar **1** was carried out at 200°C in benzene solution in sealed tubes. Monitoring the progress of small-scale runs in deuteriobenzene by ^1H NMR and high-performance liquid chromatography (HPLC) showed that the reaction proceeds to ca. 70% completion after 4 h under these conditions in each case. The products were isolated and purified by semi-preparative medium-pressure chromatography, using a combination of normal- and reverse-phase conditions. The reaction produced four main products in each case (eq. [2]), and one minor product in yields that were too low (6–7%) to enable isolation. The distribution of adducts is independent of the aryl substituent in **6–8**, within experimental error. Ene adducts **9***a* and **9***b* are formed in ca. 34 and 25% yield, respectively, ene adduct **10** is formed in ca. 13% yield, and the Diels–Alder adduct **11** is formed in ca. 20% yield. Product yields were determined by quantitative HPLC analyses. It is interesting to note that the distributions of adducts obtained from reaction of **1** with the series of *N*-aryl maleimides are very similar to that reported for the reaction of **2** with maleic anhydride (14).

Preliminary structure assignments for **9–11** (Ar = *para*-biphenyl) were made on the basis of their high-field ^1H and ^{13}C NMR spectra in deuteriochloroform solution, as well as their infrared and chemical ionization mass spectra. For each adduct, DEPT ^{13}C NMR spectra were recorded to distinguish between C/CH_2 and CH/CH_3 resonances. Heteronuclear ^1H-^{13}C shift correlated spectra, ^1H–^1H COSY, and TOCSY experiments were then recorded to establish ^1H–^{13}C and ^1H–^1H connectivities (19). The high-field ^1H and ^{13}C NMR spectra of the adducts were essentially independent of the *N*-aryl substituent, except of course in the aromatic regions.

The ^1H NMR spectra of ene adducts **9***a* and **10** and the Diels–Alder adduct **11** (Ar = phenyl) were investigated in greater detail, in an attempt to establish the differences in the structures of the B and C rings for the first two molecules, and to rigorously establish the stereochemistry of addition in the case of the third. Figure 1 shows the 500 MHz ^1H NMR spectra of **9***a* and **10**, illustrating the pronounced differences in the methyl proton resonances in the 0.8–1.3 ppm region for the two adduct types, and the slightly more subtle differences that occur elsewhere in the spectra. Figures 2 and 3 show contour plots obtained from the ^1H–^1H COSY and the ^1H–^{13}C shift-correlated spectra of adduct **9***a*, respectively. The pertinent details of our spectral assignments for compound **9***a* are presented below, along with a brief description of the assignments for **9***b*, **10**, and **11** where they differ from those of **9***a*. The ^1H and ^{13}C NMR spectra of **1** (which have been completely assigned (20)) and those of other, similar cholestane steroids (21–23) were especially helpful in deriving the spectral assignments for these compounds. It should be noted that while eq. [2] specifically identifies **9***a* as having *R* stereochemistry at C-1′ of the maleimide ring, we are actually not able to distinguish between the two diastereomers on the basis of our NMR data.

The TOCSY 2-D experiment provides a means of reveal-

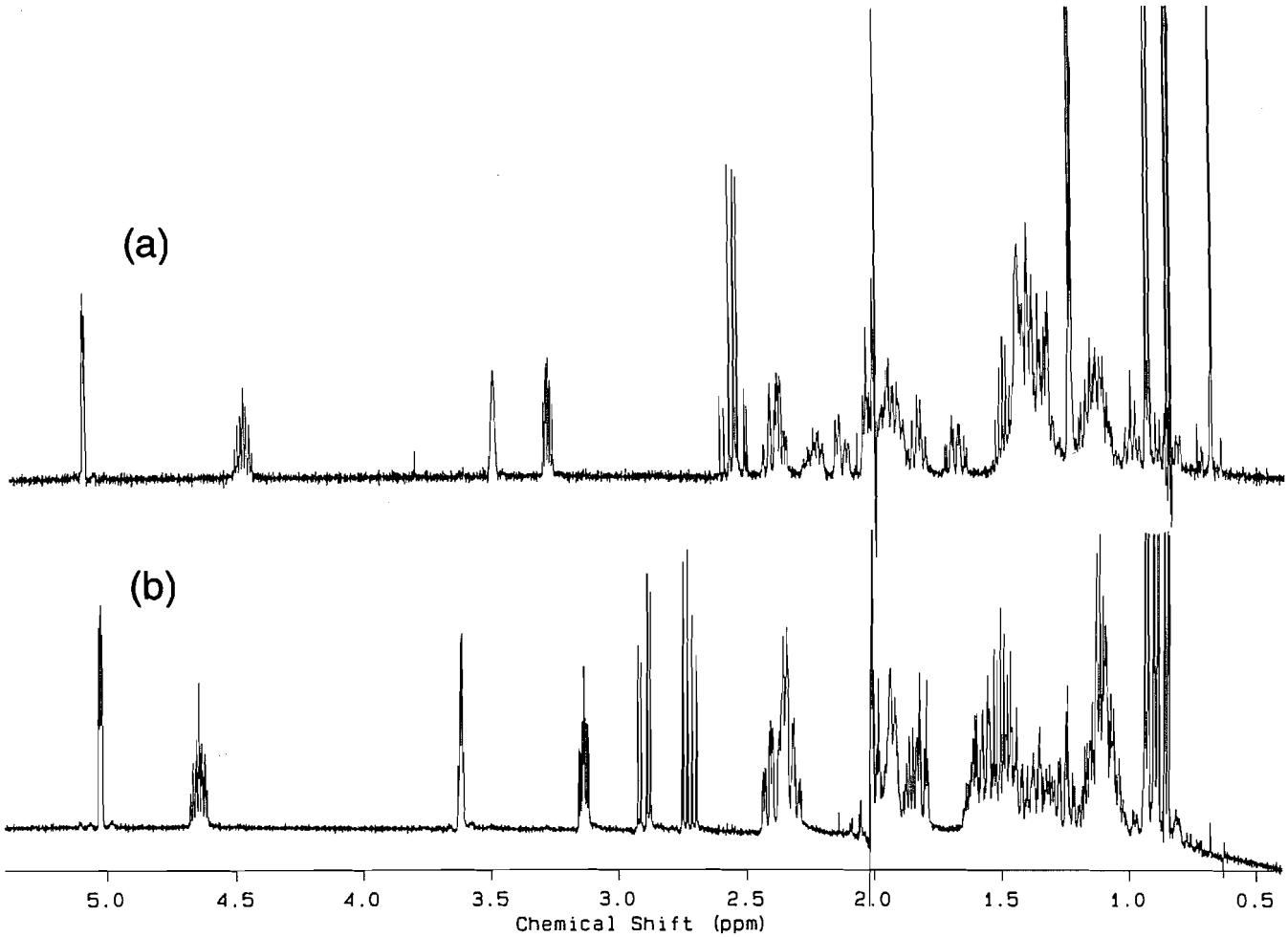

FIG. 1. High-field (500 MHz) ^{1}H NMR spectra (0–5.1 ppm region) of (*a*) **9***a* (Ar = phenyl) and (*b*) **10** (Ar = phenyl) in $CDCl_3$ solution.

ing coherence transfer throughout a spin system and will produce cross-peaks between protons that are not spin-coupled but belong to the same spin system. In principle, this technique should be able to resolve entire spin systems for specific steroid rings. To illustrate the application of the TOCSY method, Fig. 4 displays cross sections taken through the C-15 and C-3 protons of steroid **9***a*. For the former, correlations are observed not only to all the other ring-D protons but also to H-20 (overlapped by H-16α) and the 21-CH_3 protons. Similarly, all the A-ring protons were resolved by the observation of TOCSY correlations between H-3α and the C-1 protons. Figure 5 displays the TOCSY contour plot of Diels–Alder adduct **11**, obtained with an 80 ms spin-lock time.

The ^{1}H and ^{13}C NMR chemical shifts and ^{1}H–^{1}H spin coupling constants for **9***a*, **10**, and **11** (Ar = phenyl) are tabulated in Tables 1 and 2, respectively, while the results of the ^{1}H–^{1}H NOE experiments are listed in Table 3. The proton chemical shifts and coupling constants presented in Tables 1 and 2 were not refined by iterative spectral simulation. Interpretation of the information obtained from the NOE experiments was assisted by consideration of energy-minimized structures of the adducts determined from molecular mechanics (MMX) calculations. The results of these calculations are shown in Figure 6. Vicinal ^{1}H–^{1}H coupling constants, calculated from the energy-minimized structures of **9–11** using the equation included in the molecular mechanics software package (see experimental section), are included in Table 2 for comparison to the experimentally determined values. All of the adducts exhibited IR and mass spectral properties that were consistent with their proposed structures. ^{1}H and ^{13}C NMR assignments for **9***b* (Ar = *p*-biphenyl) are collected in the experimental section.

(i) Spectral assignments: ene adduct **9**a

The general strategy for assigning the ^{1}H spectrum was to begin with the olefinic proton H-6 at 5.03 ppm and H-3α at 4.65 ppm and establish both through-bond and through-space connectivities with neighbouring protons and then proceed into the adjacent ring spin systems. Through-space connectivity was provided by NOE difference experiments and this information was examined in relation to the energy-minimized structure of the molecule (Fig. 6*a*). In the COSY-45 contour plot of **9***a*, H-6 displayed cross-peaks with protons at 3.62 and 2.31 ppm. The 3.62 ppm multiplet correlates with a signal at 3.14 ppm that appears as the X part of an isolated ABX spin system arising from the C-1′ and C-2′ protons (3.14 and 2.90, 2.73 ppm, respectively) of the *N*-phenyl substituted imide ring. This dictates that the 3.62 ppm multiplet must be assigned to H-7.

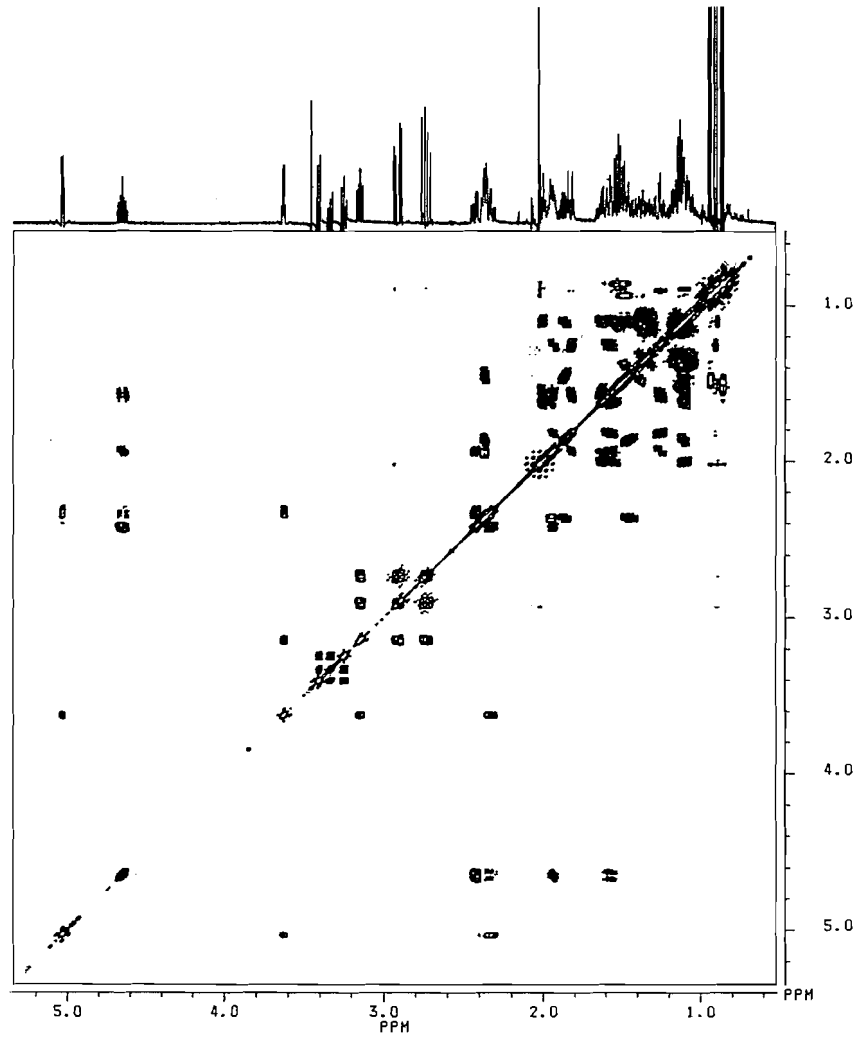

FIG. 2. COSY-45 spectrum of **9***a* in $CDCl_3$ solution.

Proton H-7 also shows a correlation with the complex multiplet at 2.31 ppm. Closer examination of the 2.31 ppm signal revealed that it overlaps with a two-proton multiplet and that it is coupled to the signal at 2.49 ppm as well as to H-3α at 4.65 ppm. Proton H-3α was also coupled to the signal at 2.49 ppm. These COSY connectivities suggest that the 2.31 and 2.49 ppm signals arise from the protons on C-4. Presumably, the cross-peaks between 2.31 ppm and H-6 and H-7 are due to long-range coupling over four and five bonds, respectively. Differentiation of the C-4 protons was achieved by NOE experiments. Saturation of the 19-CH_3 signal at 0.90 ppm resulted in an enhancement of the C-4 proton at 2.31 ppm, allowing it to be assigned to H-4β. Similarly, saturation of H-3α enhanced the H-4α signal at 2.49 ppm.

The identification of H-4β provided a means for determining if H-7 occupies an α or β position by using the stereochemical dependence of the five-bond homoallylic coupling between these protons. Maximum homoallylic coupling is observed when both coupled nuclei are 90° above or below the plane of the double bond (24). In this case with the geometry of H-4β being fixed, the 3.5 Hz five-bond coupling can only arise with H-7 being in a β position as shown in Fig. 6*a*. Furthermore, in an NOE experiment where H-7 was saturated there was an enhancement of a multiplet later identified as H-15α,β. This NOE result can be accounted for provided H-7 is in the β position. The structure in Fig. 6*a* indicates an average internuclear distance of 2.4 Å between H-7β and H-15α,β. During this NOE experiment H-6 and H-1′ were also enhanced.

The assignment of the A-rings protons was completed by following the cross-peaks in the COSY-45 spectrum from H-3α to the multiplets corresponding to the C-2 protons (1.93 and 1.57 ppm) and then from the C-2 protons to the C-1 methylene protons at 1.25 and 1.82 ppm. The α and β protons were identified in an NOE experiment where the 19-CH_3 was saturated (Tables 1 and 3). Additional confirmation of the H-2α assignment was provided by the observation of a four-bond W-type coupling (2.2 Hz) between H-4α and H-2α. A four-bond coupling was also detected between H-1α and the 19-CH_3 in the COSY spectrum.

Only a limited number of protons on the C and D rings and on the C-17 side chain could be identified from the ^1H spectrum because of the high degree of signal overlap in the 0.5–1.7 ppm region. A four-bond coupling resulted in a cross-peak being observed in the COSY-45 between the 18-CH_3 and H-12α (1.10 ppm) protons. Methyls 26 and 27 correlated with the H-25 multiplet centred at 1.51 ppm. Proton

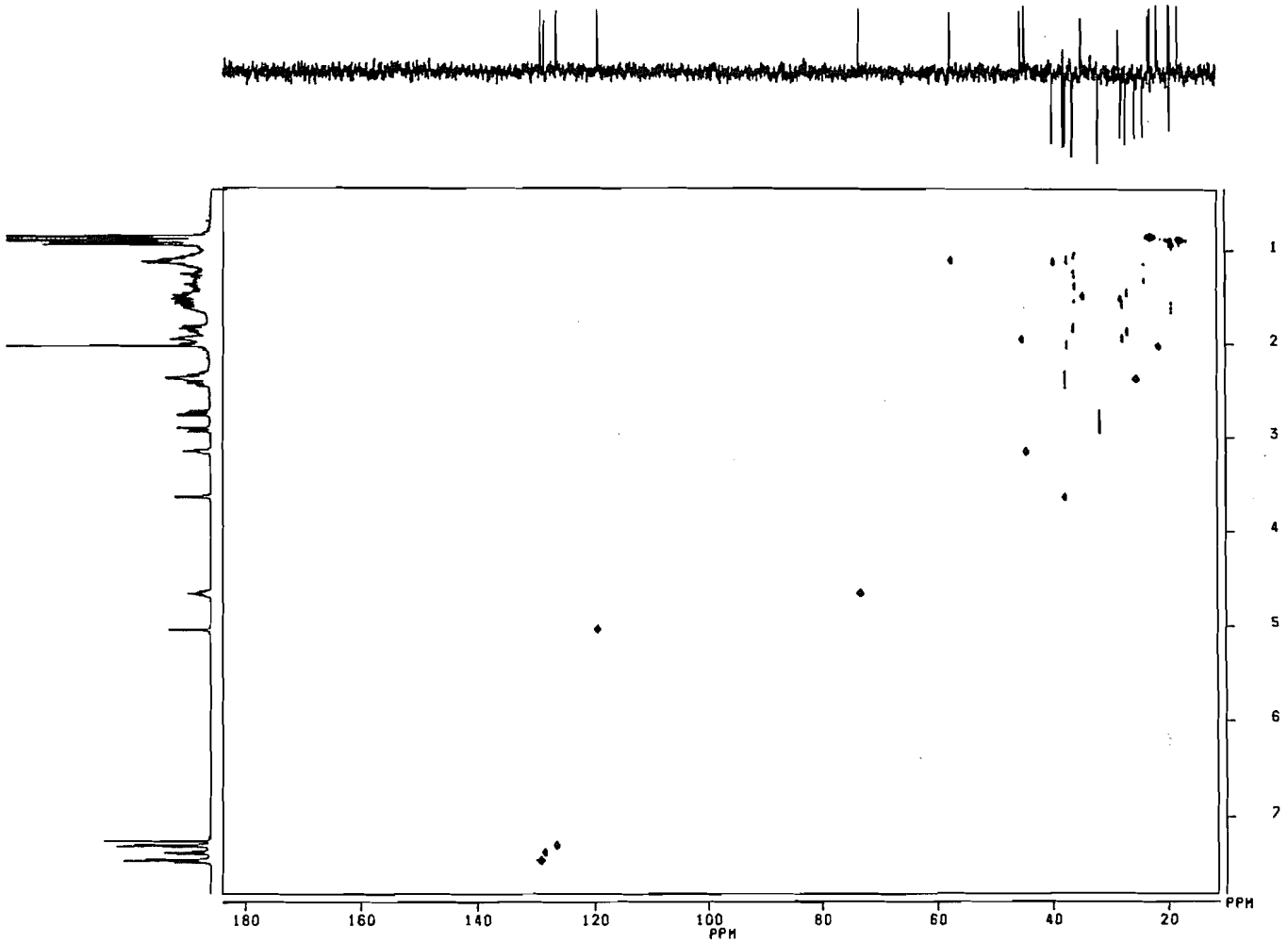

FIG. 3. $^{1}H-^{13}C$ shift correlation spectrum of **9***a* in $CDCl_3$ solution. The ^{13}C spectrum is shown as the DEPT spectrum.

H-20 was assigned to 1.48 ppm on the basis of its correlation with the 21-CH_3 doublet at 0.93 ppm.

The $^{1}H-^{13}C$ 2-D shift correlation experiment allows assignment of the remaining proton resonances and facilitates the analysis of the ^{13}C spectrum. A preliminary assignment of the ^{13}C NMR spectrum (Table 1) was achieved by the DEPT technique and by comparison with literature data (22, 23). Olefinic carbons 5 and 6 could be readily assigned by these methods to 145.9 and 119.3 ppm, respectively. However, the assignment of carbons 8 and 14 remains tentative.

Cross sections from the shift correlation spectra were particularly useful for assigning both the aliphatic carbons and their corresponding directly bonded protons. Since the A-ring protons were already identified, this simplified the assignment of carbons 1 through 4 (Table 1). There was an overlap of the C-4 and C-7 resonances. In the C ring, the previously assigned H-12α (1.10 ppm) was correlated with the carbon at 37.3 ppm. The cross section through this carbon resonance located H-12β (2.00 ppm), which was overlapped by the acetate methyl singlet. The C-11 methylene protons (1.63 and 1.53 ppm) were revealed in the COSY-45 spectrum by the cross-peaks with the C-12 protons. The C-11 carbon (19.1 ppm) was difficult to assign because of overlap with the 19-CH_3.

The resolution of the methine carbon signals between 40 and 75 ppm made it possible to assign the H-17α and H-9α protons (Table 1), which were obscured in the ^{1}H NMR spectrum. Identification of H-17α provided the means for assigning the other D-ring protons since a cross-peak was detected in the COSY spectrum to the multiplet eventually assigned to H-16β (1.83 ppm). The combination of the COSY and shift correlation data indicated that the C-16 methylene protons were at 1.83 and 1.46 ppm. Their designation as α (1.46 ppm) and β (1.83 ppm) is tentatively based on the coupling constants estimated from these multiplets (Table 3) (19, 22). However, it should be noted that this method of assignment is considered controversial (21). Both C-16 protons show correlations with an unresolved multiplet overlapping H-4β at 2.36 ppm; by elimination, this multiplet can be assigned to the H-15α,β protons. In the cross section through the shift correlation spectrum, H-15α,β appeared as a singlet connected to the carbon at 25.2 ppm, indicating that these methylene protons are in fact equivalent. The assignment of the C-17 side-chain protons and carbons relied on the COSY and shift correlation spectra and comparisons with literature data.

The TOCSY 2-D experiment, which produces cross-peaks between protons that are not coupled but belong to the same spin system, provided additional confirmation of some of the ^{1}H assignments. In particular, all the A-ring protons

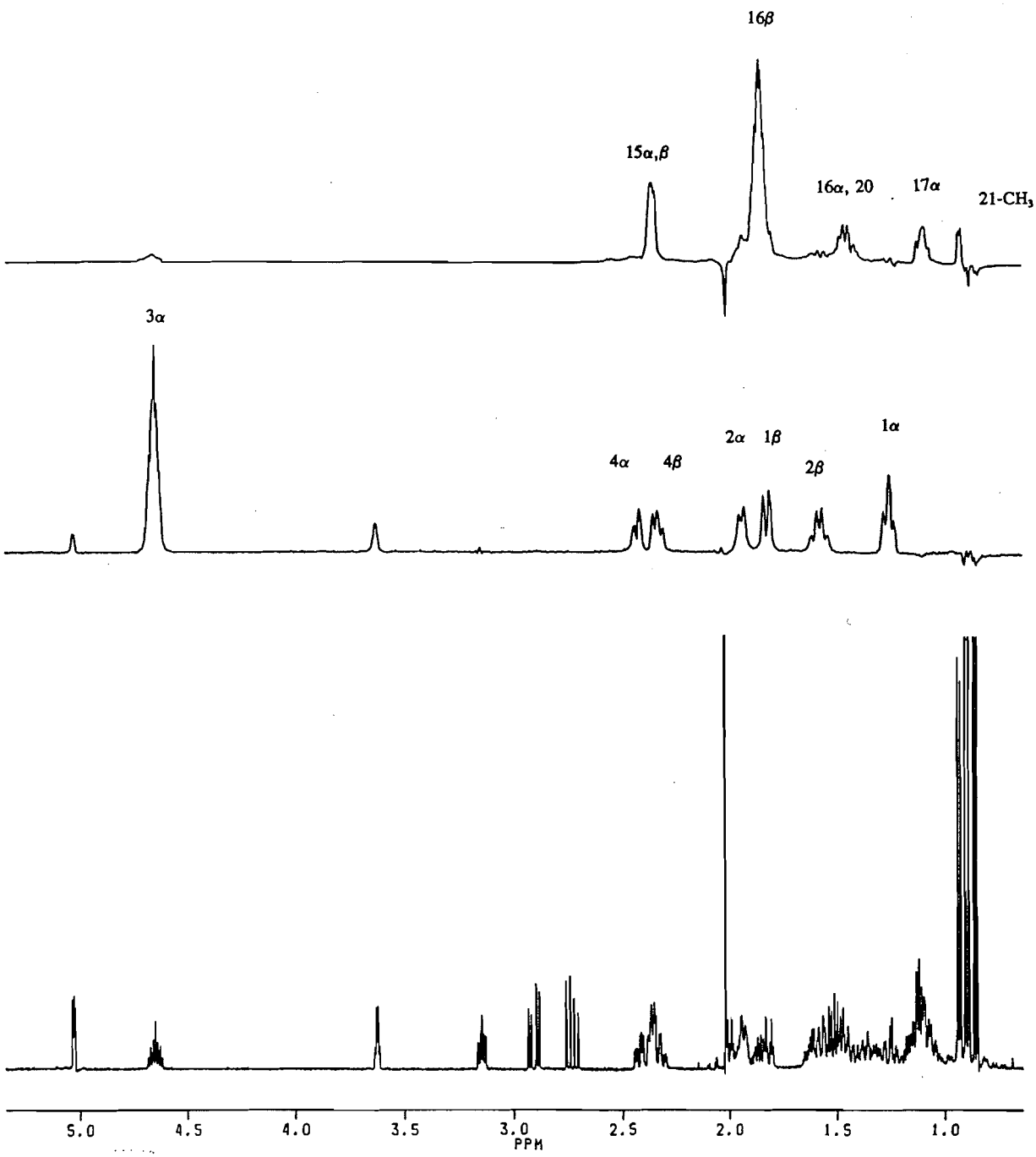

FIG. 4. Cross sections taken from the TOCSY spectrum of adduct **9***a* showing the resolution of the protons in rings A and D (middle and top spectra, respectively). The correlation between H-15α,β and the 21-CH_3 indicate coherence transfer occurring over six bonds.

could be identified by taking a cross section through the H-3α signal. In addition to the normal correlations with the C-2 and C-4 protons, H-3α also shows TOCSY cross-peaks to the C-1 protons at 1.25 and 1.82 ppm. An interesting result was the observation of TOCSY correlations through the entire D-ring spin system between 21-CH_3 and the C-15 protons (Fig. 4, top). In the cross section through 21-CH_3, the only proton not clearly observed was H-20, which was overlapped with the multiplet from H-16α. The H-15 to 21-CH_3 proton correlation indicates coherence transfer occurring between nuclei separated by six bonds. Unfortunately, the H-9/H-11/H-12 correlation could not be clearly observed due to overlap of the broad H-9 proton resonance with other signals.

(ii) Spectral assignments: ene adduct **9**b

The ^1H and ^{13}C spectra of **9***b* appear to be somewhat different from those of **9***a*, though they are essentially identical in the 0.8–1.0 ppm (methyl) regions. ^1H–^1H COSY and ^1H–^{13}C shift-correlated spectra of **9***b* (Ar = biphenyl), made in identical fashion to those for **9***a* (*vide supra*), allow sufficiently detailed assignment of the ^1H spectrum to conclude that the main differences between the spectra of **9***a*,*b* are associated with the B-ring carbons (C-6–C-9) and their corresponding protons. This is consistent with the identifi-

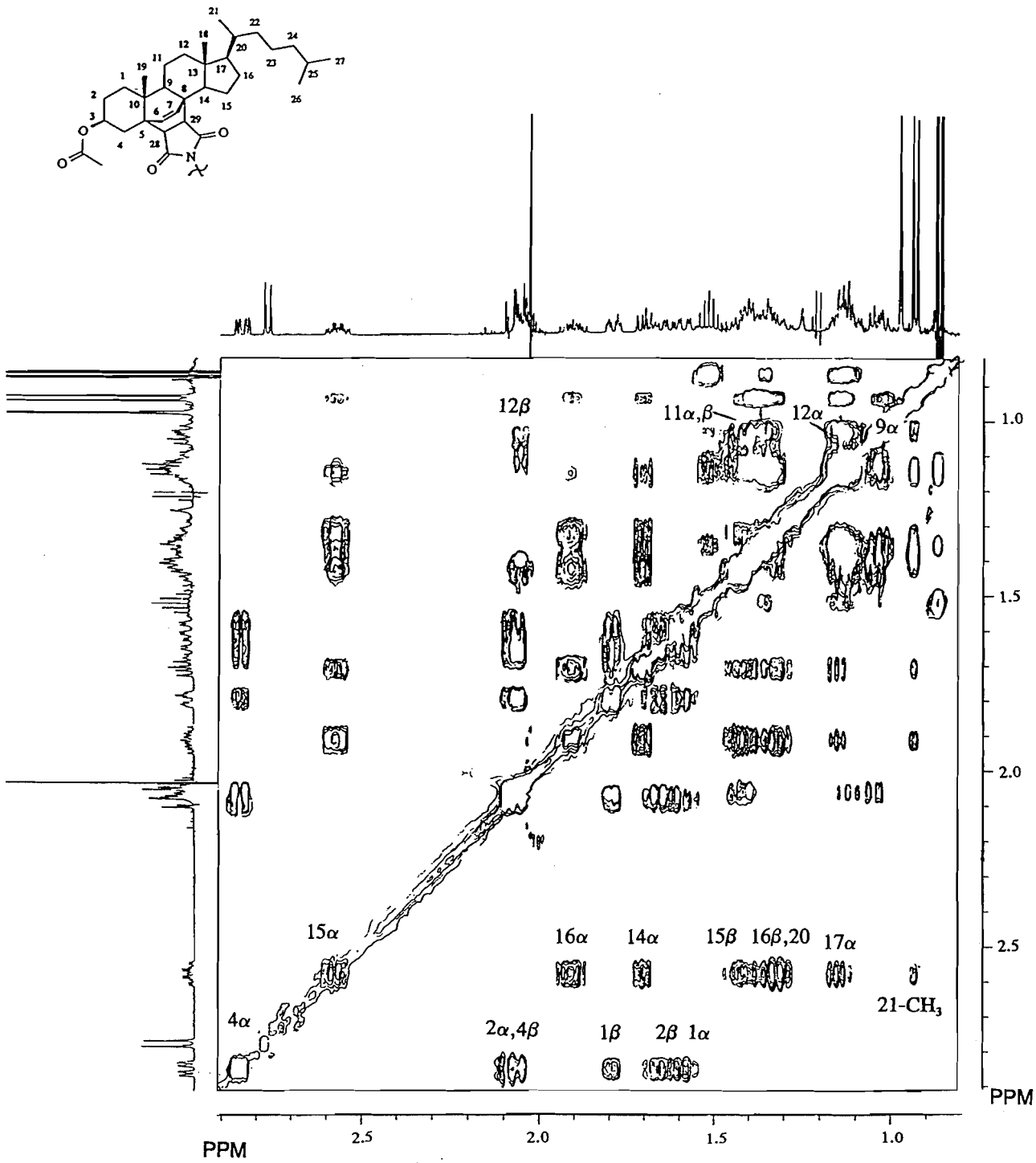

FIG. 5. TOCSY contour plot of the region from 0.8 to 2.9 ppm for adduct **11** (Ar = phenyl), recorded with an 80 ms spin-lock time.

cation of **9***a* and **9***b* as diastereomers differing only in the stereochemistry at the 1′-position of the maleimide ring. In the ^{1}H NMR spectrum of **9***b*, H-6 appears at 5.51 ppm (cf. 5.03 ppm in **9***a*), H-7β appears at 3.16 ppm (cf. 3.62 ppm in **9***a*), and H-9α appears at 2.25 ppm (cf. 1.94 ppm in **9***a*). Also, the H-15 protons are shifted to 2.17 and 2.27 ppm, from their position of 2.36 in **9***a*. The remaining protons in **9***b* appear within 0.06 ppm of their positions in the spectrum of **9***a*.

The main differences in the ^{13}C spectrum are due to C-5 (143.6 ppm), C-6 (121.5 ppm), C-7 (39.9 ppm), C-8 (125.9 ppm), and C-9 (44.0 ppm), to be compared with the corresponding resonances in **9***a* (145.9, 119.3, 37.6, 132.0, and 45.1 ppm, respectively). Also, the C-1′ and C-2′ resonances are shifted to 45.7 and 33.9 ppm, respectively, from their positions in the spectrum of **9***a*. The remaining resonances in the ^{13}C NMR spectrum of **9***b* are within 0.4 ppm of their positions in the spectrum of **9***a*.

The assigned ^{1}H and ^{13}C resonances for this compound are listed in the experimental section.

TABLE 1. ^1H and ^{13}C chemical shifts for **9a**, **10**, and **11** from NMR spectra in $CDCl_3$[a]

	9a Chemical shift (ppm)		**10** Chemical shift (ppm)		**11** Chemical shift (ppm)	
C/H	^1H	^{13}C	^1H	^{13}C	^1H	^{13}C
1	1.25(α), 1.82(β)	36.0	1.40(α), 2.03(β)	36.2	1.56(α), 1.77(β)	34.5
2	1.93(α), 1.57(β)	27.7	1.96(α), 1.68(β)	27.7	2.04(α), 1.64(β)	26.7
3	4.65(α)	73.1	4.49(α)	74.1	5.30(α)	69.5
4	2.49(α), 2.31(β)	37.6	2.38(α), 2.42(β)	38.2	2.83(α), 2.05(β)	31.3
5	—	145.9	—	143.1	—	45.8[d]
6	5.03	119.3	5.11	117.5	5.81	135.7
7	3.62(β)	37.6	3.51(β)	38.9	6.22	130.5
8	—	132.0	—	126.2	—	44.9[d]
9	1.94(α)	45.1	—	136.5	1.03(α)	53.4
10	—	38.5	—	38.4	—	40.8[d]
11	1.63(α), 1.53(β)	19.1	2.13(α), 2.26(β)	22.8	1.39(α), 1.39(β)	22.8[d]
12	1.10(α), 2.00(β)	37.3	1.42(α), 1.96(β)	28.7	1.10(α), 2.05(β)	39.5
13	—	43.2	—	42.3	—	43.6[d]
14	—	125.3	1.92(α)	50.2	1.68	54.8
15	2.36(α), 2.36(β)	25.2	1.84(α), 1.42(β)	23.4	2.55(α), 1.40(β)	23.1
16	1.46(α), 1.83(β)	26.8	1.18(α), 1.92(β)	36.5	1.89(α), 1.30(β)	27.7
17	1.10(α)	57.4	1.19(α)	54.2	1.12	55.1
18-CH_3	0.89	17.8	0.69	11.6	0.73	12.4
19-CH_3	0.90	19.1	1.25	23.6	0.96	18.6
20	1.48	34.5	1.40	36.0	1.35	35.3[d]
21-CH_3	0.93	19.2	0.94	19.0	0.91	19.1
22	1.36, 1.03	36.0	1.36, 1.01	36.1	1.12, 1.35	36.0[d]
23	1.32, 1.14	23.8	1.34, 1.15	23.8	1.12, 1.35	23.8[d]
24	1.12	39.5	1.12	39.5	1.12, 1.35	38.9[d]
25	1.51	28.0	1.51	28.0	1.50	28.0
26, 27	0.86, 0.85	22.6, 22.8	0.86, 0.85	22.8, 22.5	0.85	22.8, 22.5
CH_3CO	2.02	21.3	2.01	21.3	2.01	21.9
CH_3CO	—	170.4	—	[c]	—	[c]
1′	3.14	44.4	3.29	42.9	3.38	42.3
2′	2.90, 2.73	31.5	2.59, 2.55	30.2	2.75	56.6
3′	—	175.7[b]	—	178.1	—	[c]
4′	—	177.8[b]	—	[c]	—	[c]

[a]Aromatic protons appeared in the 7.29–7.44 ppm range; aromatic carbons in the 126.4–147 ppm range.
[b]Assignments may be reversed.
[c]Signals not observed due to low sample concentration.
[d]Assignments tentative.

*(iii) Spectral assignments: ene adduct **10***

The chemical shifts and coupling constants for **10** were determined using procedures similar to those used for **9a**. The ^1H and ^{13}C spectral assignments presented for this compound in Table 1 should be viewed with greater caution than those for **9a**, since there was considerably greater overlap of signals in the ^1H spectrum of **10** and only a small number of coupling constants could be determined reliably. However, sufficient resolution was obtained to confirm the stereochemistry at C-7 and to give an indication of the change in position of the second double bond in ring B.

By analogy with the data for **9a**, the homoallylic coupling (2.1 Hz) is consistent with H-7 occupying a β position. Therefore, the stereochemistry at C-7 in **10** appears to be the same as that in **9a**.

The position of the C-8/C-9 double bond was determined by locating the C-11 protons and examining their geminal coupling. These protons (11α, 2.26 and 11β, 2.13 ppm) were identified in the COSY-45 spectrum and were differentiated in an NOE experiment where the 19-CH_3 was saturated. An evaluation of the geminal coupling from the H-11α multiplet showed it to be approximately −18.1 Hz. The substantial increase in the magnitude of the geminal coupling is consistent with the plane of the π-system bisecting the angle between the C-11 methylene protons (25–27). This result confirms that the double bond is in fact located between C-8 and C-9.

*(iv) Spectral assignments: Diels–Alder adduct **11***

The gross structure of the Diels–Alder adduct (**11**) is particularly easy to identify because of the AX patterns in the ^1H NMR spectrum due to the vinylic protons at C-6 and C-7 (5.81 and 6.22 ppm, respectively) and the maleimide protons at C-1′ and C-2′ (2.75 and 3.38 ppm, respectively). Assignment of the A- and C-ring protons (Table 1) was achieved by a combination of COSY-45 and TOCSY (Fig. 5) 2-D techniques as well as NOE difference spectra (Table 3). The C-ring assignments were complicated by the overlap of H-11α and H-11β.

The B-ring vinyl proton chemical shifts were assigned with the aid of NOE difference spectra in which the methyl signals at 0.73 and 0.96 ppm were saturated. In the experiment where the 0.93 ppm methyl resonance was irradiated, an enhancement of the 5.81 ppm doublet was observed.

TABLE 2. Observed and calculated[a] ^1H–^1H coupling constants (±0.5–1.0 Hz) for **9a**, **10**, and **11** in $CDCl_3$

	9a		**10**		**11**	
Protons	^2J	^3J	^2J	^3J	^2J	^3J
1α, 1β	−13.8		—		−13.2	
1α, 2α		3.8(3.6)		—		3.4(4.3)
1α, 2β		13.9(13.6)		13.3(13.4)		13.4(13.2)
1β, 2α		3.8(3.3)		—		3.2(2.7)
1β, 2β		3.8(3.2)		4.4(3.7)		3.2(4.1)
2α, 2β	−12.9		−13.3		−12.5	
2α, 3α		4.7(4.2)		—		5.2(5.5)
2β, 3α		11.6(11.4)		11.7(11.1)		11.6(10.6)
4α, 4β	−13.9		−12.4		−13.0	
4α, 3α		5.1(4.6)		5.6(4.9)		4.9(4.7)
4β, 3α		11.6(11.1)		12.0(10.7)		12.3(10.7)
6, 7		3.8(3.8)		3.3(3.6)		8.6
9α, 11α		7.2(7.3)		—		6.2(4.3)
9α, 11β		10.2(9.9)		—		11.9(12.0)[b]
11α, 11β	−14.1		−18.1			
11α, 12α		3.4(3.4)		—		4.8(3.4)[b]
11α, 12β		3.4(3.3)		—		
11β, 12α		14.0(13.2)		—		12.5(13.2)
11β, 12β		3.4(3.9)		—		3.7(4.0)
12α, 12β	−12.8		—		−12.5	
14α, 15α		—				7.2(6.0)
14α, 15β		—		—		12.3(11.5)
15α, 15β	—		—		−12.5	
15α, 16α		9.4[c](9.9)		—		10.6(11.7)
15α, 16β		5.9[c](8.6))		—		3.0(2.4)
15β, 16α		—		—		6.0(4.6)
15β, 16β		—		—		12.2(11.8)
16α, 16β	−13.3		—		−11.6	
16α, 17α		7.5(5.1)		—		9.5(6.8)
16β, 17α		12.9(12.0)		—		9.5(10.8)
17α, 20			—		—	9.5

[a]Calculated from the energy minimized structures (Fig. 6), using the equation supplied with PCModel Version 4.0. Calculated values are in parentheses following the observed values.
[b]Overlapping multiplets; coupling not resolved.
[c]Assignment uncertain.

Several other protons arising mainly from ring A were also enhanced (Table 3). Thus, the 0.93 ppm singlet must be assigned to the 19-CH_3 while the vinylic doublet at 5.81 ppm can be attributed to H-6. Saturation of the 18-CH_3 resonance (0.73 ppm) produced the corresponding enhancement of H-7 (6.22 ppm) (Table 3). These NOE results provide experimental verification of the agreement of our assignments of the C-18 and C-19 methyl resonances with those of Jones *et al.* for the Diels–Alder adduct from **2** and maleic anhydride (14). In addition, the NOE data also confirm the *endo*- stereochemistry of adduct **11** as shown in the MMX-derived structure in Fig. 6*c*. Methyl-19 is close to H-6 while the 18-CH_3 is in the proximity of H-7. Further support for this geometry was provided by NOE experiments that involved the saturation of H-1′ and H-2′ protons of the succinimidyl ring. Saturation of the 3.38 ppm signal produced an enhancement of H-3α at 5.30 ppm, thereby allowing the 3.38 ppm resonance to be assigned to H-1′. The neighbouring H-2′ proton (2.75 ppm) was enhanced along with the 1.56 ppm H-1α multiplet. Saturation of H-2′ resulted in NOE's to H-1′ and to the 1.03 ppm multiplet assigned to H-9α.

The D-ring protons were identified from the COSY-45 and TOCSY (Fig. 5) spectra. The isolated multiplet at 2.55 ppm correlates with the doublet of doublets at 1.68 ppm and with the multiplets at 1.89, 1.40, and 1.30 ppm. Measurement of the coupling constants for the 2.55 and 1.68 ppm multiplets indicated a 7.2 Hz coupling between these protons. The remaining 12.3 Hz coupling associated with the 1.68 ppm signal arises from an interaction with the proton at 1.40 ppm. These results were interpreted with H-14α being assigned to 1.68 ppm with an axial/pseudo-equatorial coupling (7.2 Hz) to H-15α (2.55 ppm), and an axial/pseudo-axial coupling (12.3 Hz) to H-15β (1.40 ppm). The 1.89 and 1.30 ppm signals were shown by NOE experiments involving saturation of H-15α (Table 3) to arise from H-16α and H-16β, respectively. The D-ring proton H-15β was also affected by saturation of the olefinic proton H-7 (6.22 ppm). This enhancement is consistent with the spatial geometry of these protons as shown in the MMX structure (Fig. 6*c*).

The TOCSY contour plot (Fig. 5) allowed the completion of the D-ring assignments by the observation of the correlation between H-15α and H-17α. The longer-range correlation was also detected between H-15α and the 21-CH_3 protons. The multiplet for H-20 was not observed because of overlap with the H-15β and H-16β signals.

TABLE 3. Summary of NOE experiments for **9*a***, **10**, and **11**

Compound	Saturated (ppm)	Enhanced (%[a])
9*a*	3α (4.65)	4α (5.8%), 2α (3.9%)
	6 (5.03)	4α (6.0%), 7β (8.4%)
	19-CH_3 (0.90)	1β (1.9%), 2β (9.9%), 4β (3.0%)
	7β (3.62)	6 (7.9%), 1′ (5.0%), 15 (3.6%)
10	19-CH_3 (1.25)	1β (1.8%), 4β (3.3%), 11β (2.7%)
	6 (5.11)	4α (3.4%), 7β (4.9%)
11	18-CH_3 (0.73)	7 (7.3%), 11β (18.0%)
	19-CH_3 (0.96)	6 (2.2%), 11β (12.0%), 4β (8.8%), 2β (2.0%), 1β (0.5 %)
	1′ (3.38)	2′ (4.5%), 3α (8.3%), 1α (3.2%)
	2′ (2.75)	1′ (4.6%), 9α (5.8%)
	6 (5.81)	7 (6.5%)
	7 (6.22)	6 (8.2%), 15β (4.7%)
	15α (2.55)	15β (17.9%), 16α[b]

[a]Intensities measured from the difference spectrum are reported relative to the saturated signal where the intensity was assigned to −100 for a single proton multiplet; the peaks of interest were then integrated. Since the samples were not degassed, these results cannot be considered quantitative and serve only as a general indication of the observed enhancement of the signals. For the applications in this study, the determination of a numerical value for the NOE was not critical since the detection of an enhancement in itself is sufficient to provide the required structural information (40).

[b]The percent change in peak intensity is not considered accurate due to overlap with other signals or baseline distortions resulting from incomplete subtraction of adjacent peaks.

Only a partial assignment of the alkyl side-chain protons was possible from the 2-D spectra. The 26,27-CH_3 protons displayed TOCSY cross-peaks to contours centered at 1.35 and 1.12 ppm. These cross-peaks are considered to arise from the protons on carbons 22, 23, and 24, but no further differentiation of these signals was possible.

Summary and conclusions

The reaction of 7-dehydrocholesteryl acetate (**1**) with *N*-aryl maleimides yields mixtures of ene and Diels–Alder adducts. There is very little variation in the relative yields of the adducts with *N*-aryl substituent throughout the series **6–8**, and the product distributions are similar to that reported previously for the reaction of ergosteryl acetate with maleic anhydride (14).

The structures of the ene-adducts **9** and **10** and Diels–Alder adduct **11** from the reaction of **1** and **6–8** have been elucidated by high-field ^1H and ^{13}C NMR spectroscopic techniques, employing 2-D chemical shift correlation experiments and molecular mechanics calculations to assist in the spectral assignments. The accuracy with which the latter is able to predict coupling constants in these systems is quite remarkable. In all cases, the present assignments verify the conclusions of previous workers, who employed differences in the chemical shifts of the C-18 and C-19 methyl protons to identify the structures of the various adduct types (1–4).

TOCSY spectra have been reported previously for a triterpenoid (39). However, to our knowledge, the present work represents one of the first demonstrations of the power of the TOCSY pulse sequence for resolving entire spin systems in steroids. This technique will undoubtedly find increasingly frequent use in the analysis of the ^1H NMR spectra of complex natural products.

Experimental

Melting points were determined using a Mettler FP82 hot stage (controlled by a Mettler FP80 central processor) mounted on an Olympus BH-2 microscope, and are corrected. Routine ^1H NMR spectra were recorded with Varian EM390 or Bruker AC200 NMR spectrometers, and referenced with internal tetramethylsilane. Infrared spectra were recorded as KBr pellets (except where noted otherwise) using a Perkin–Elmer model 283 infrared spectrometer, calibrated with the 1601.8 cm^{-1} polystyrene absorption. Mass spectra and exact masses were determined by electron impact (70 eV), using a VG analytical ZAB-E mass spectrometer with a source temperature of 200°C and direct probe injection. Combustion analyses were performed by Galbraith Laboratories, Inc.

Analytical high-performance liquid chromatographic analyses employed a Gilson Isocratic HPLC system consisting of a model 302 pump and 5-mL head, a model 802B manometric module, Holochrome variable wavelength detector, and a Rheodyne model 7125 loop injector. A detector wavelength of 235 nm was used for analysis of product mixtures from reaction of **1** and **6**. Analyses of those from reaction of **1** with **7** and **8** employed a detector wavelength of 280 nm. The detector was interfaced with a Unitron microcomputer (Apple II+ clone) through an Adalab® data acquisition/control card (Interactive Microware, Inc.). The 0–10 mV signal was amplified to 0–1 V using an Adaamp® analog amplifier (Interactive Microware, Inc.). Chromatogram acquisition and storage was performed using Chromatochart® (Interactive Microware, Inc.). Product yields were determined from the HPLC peak areas (calculated by triangulation), assuming identical detector responses for each set of adducts and are the averages of two runs each analysed in triplicate. Normal-phase separations employed a Merck Hibar (4.6 × 220 mm) Si60 (10 μm) column, while reverse-phase separations employed Alltech (4.6 × 250 mm) C18 (10 μm) or Brownlee (4.6 × 220 mm) RP-18 Spheri-10 columns.

Semi-preparative LC separations were performed with the above system equipped with a 50-mL recycling pump head and an Isco 254-nm single wavelength detector. Normal-phase separations were performed with an EM Lobar Si60 (2.5 × 25 cm) silica column,

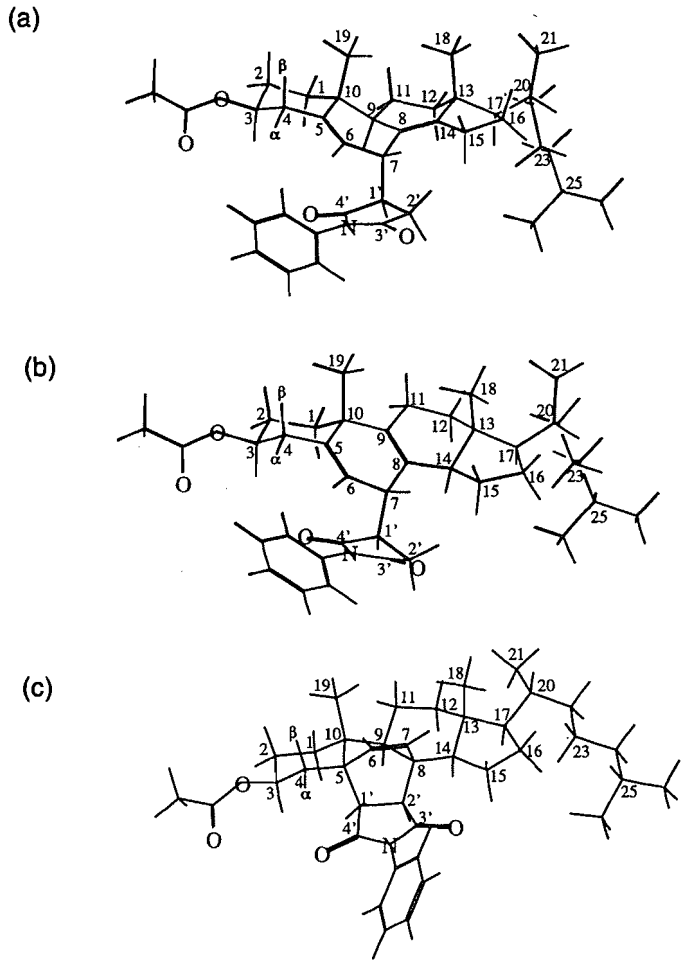

FIG. 6. Energy-minimized (MMX) structures of adducts **9***a* (*a*), **10** (*b*), and **11** (*c*).

while reverse-phase separations were performed using a Whatman Partisil M9 10/50 ODS-2 column.

High-resolution ^{1}H and ^{13}C NMR spectra were recorded on a Bruker AM500 spectrometer. Proton spectra were acquired at 500.135 MHz using a 5-mm dual frequency ^{1}H–^{13}C probe. Spectra were obtained in 64–88 scans in 32K data points over a 2.415–3.012 kHz spectral width (5.439–6.783 s acquisition times). The sample temperature was maintained at 30°C by a Bruker BVT-1000 variable temperature unit. The free induction decay (FID) was processed using Gaussian multiplication (line broadening: −2.0 Hz, Gaussian broadening factor: 0.15) for resolution enhancement and was zero-filled to 64K before Fourier transformation.

Absolute value proton COSY 2-D NMR spectra were recorded using the pulse sequence 90°–t_1–45°–ACQ. Spectra were acquired in 32 scans for each of the 512 FID's that contained 2K data points in F2 over the previously mentioned spectral widths. The ^{1}H 90° pulse width was 18.6 μs. A 2.0 s relaxation delay was employed between acquisitions. Zero-filling in F1 produced a 1K × 1K data matrix with a digital resolution of 2.359 or 2.941 Hz/point in both dimensions. During 2-D Fourier transformation a sine-bell squared window function was applied to both dimensions. The transformed data were then symmetrized.

TOCSY 2-D NMR spectra were acquired in the phase-sensitive mode using the MLEV-17 pulse sequence (28). Phase-sensitive data were obtained using time-proportional phase incrementation (TPPI) (29, 30). In the F2 dimension, 2K data points were used during the acquisition of the 256 FID's. Each FID was acquired in 16 scans for adduct **9***a* and 176 scans for **10**. A 2.415 kHz spectral width in the F2 dimension was used for both samples. The relaxation delays were 1.0 s for **9***a* and 0.7 s for **10**. The 90° ^{1}H pulse width used in the 5-mm broadband inverse probe was 26.0 μs. The length of the spin-lock mixing time was 80 ms plus two trim pulses of 2.5 ms. Zero-filling in the F1 dimension to 2K data points resulted in a digital resolution of 2.359 Hz/point in both dimensions. During the 2-D Fourier transformation, a sine-bell squared window function shifted by $\pi/2$ was applied to both dimensions. The transformed data were not symmetrized.

Proton–proton NOE difference spectra were acquired by subtraction of a control FID from an on-resonance FID. The decoupler in the control FID irradiated a position in the spectrum where there were no proton signals. The on-resonance FID was obtained with the proton of interest being selectively saturated. In both cases the same decoupler power and duration of saturation (5.0 s) were used. This saturation period also served as the relaxation delay for both the control and on-resonance FID's. The decoupler was gated off during acquisition. Eight scans were acquired for both the control and on-resonance FID's. The cycle of alternate acquisition of control and on-resonance FID's was repeated 8 times for a total of 64 scans for the complete difference FID. A 90° ^{1}H pulse width of 18.6 μs was used. The difference FID was processed using exponential multiplication (line broadening: 4.0 Hz) and was zero-filled to 32K before Fourier transformation. Samples were not degassed.

Carbon-13 NMR spectra were recorded at 125.759 MHz using the 5-mm dual frequency ^{1}H–^{13}C probe. The spectra were acquired over a 21.739 or 30.0 kHz spectral width in 16K or 32K data points (0.377–0.557 s acquisition time). Single pulse spectra used a ^{13}C pulse width of 2.5 μs (30° flip angle) and a 0.5 s relaxation delay. The DEPT pulse sequence was used for editing. The ^{13}C 90° pulse width was 6.4 μs while the ^{1}H 90° pulse width through the decoupler channel was 18.6 μs. The delays used in the DEPT pulse sequence were a 1.0 s relaxation delay and $1/2^1J_{CH}$ delay of 0.003571 s. The FID's were processed using exponential multiplication (line broadening: 4.0–5.0 Hz).

The ^{13}C–^{1}H 2-D chemical shift correlation spectra of **9** and **10** (Ar = phenyl) were acquired using the standard pulse sequence incorporating the BIRD pulse during the evolution period for ^{1}H–^{1}H decoupling in F1 (31–33). The spectra in the F2 (^{1}H) dimension were recorded over a spectral width of 3.106 kHz in 2–4K data points. The 256–512 FID's in the F1 (^{13}C) dimension were obtained over a 19.231 kHz spectral width. Each FID was acquired in 32 scans. The fixed delays in the pulse sequence were a 0.75–1.0 s relaxation delay, BIRD pulse and polarization transfer delays ($1/2^1J_{CH}$) of 0.003571 s, a refocussing delay ($1/4^1J_{CH}$) of 0.001786 s, and a 0.3 s delay between the BIRD pulse and the inverse pulse sequence. The 90° ^{1}H pulse was 9.2 μs while the 90° ^{13}C pulse was 10.1 μs. The data for **9** and **10** (Ar = phenyl) were processed using exponential multiplication (line broadening: 11.0 Hz) in F2 and unshifted sine bell in F1. Zero-filling in F1 resulted in a 2K × 1K data matrix.

The ^{1}H–^{13}C inverse detected shift correlation spectrum of **11** was acquired by using the HMQC pulse sequence with the BIRD pulse (34) in a 5-mm broadband inverse probe. The data were obtained in the phase sensitive mode using time-proportional phase incrementation (TPPI) (29, 30). The spectra in F2 were recorded over a spectral width of 2.415 KHz in 2K data points. In F1, each of the 186 FID's was acquired in 144 scans over the ^{13}C spectral width of 14.286 KHz. The fixed delays in the pulse sequence were a relaxation delay of 0.6 s, a BIRD pulse delay ($1/2^1J_{CH}$) of 0.003571 s, and the delay between the BIRD pulse and the HMQC pulse sequence was 0.35 s. The 90° ^{1}H pulse was 8.5 μs while the ^{13}C 90° pulse was 10.3 μs. Carbon-13 decoupling during acquisition was achieved by the GARP method (35). The data were processed using a sine-bell squared window function shifted by $\pi/2$ in both dimensions. In F1, the 2-D data were zero-filled to 2K.

The compounds used in the NMR experiments were dissolved in $CDCl_3$ (MSD Isotopes) to a concentration of about 0.05 M. Chemical shifts for the ^1H and ^{13}C spectra are reported in ppm relative to TMS using the residual solvent signals at 7.24 and 77.0 ppm as internal references for the ^1H and ^{13}C spectra, respectively.

Molecular mechanics calculations employed the MMX package supplied with PCModel Version 4.0 (Serena Software, Inc). Vicinal ^1H–^1H coupling constants were calculated using the equation supplied with the same software package, from the energy-minimized structures.

HPLC solvents acetonitrile (Caledon HPLC), dichloromethane (Caledon HPLC), ethyl acetate (BDH Reagent), and hexane (Caledon HPLC) were used as received from the suppliers, as were methanol (Mallinckrodt anhydrous), acetic anhydride (BDH Reagent), 1-nitropropane (Eastman), chlorobenzene (Fisher Reagent), toluene (Caledon Reagent), and carbon tetrachloride (Caledon Reagent or Fisher Spectroscopic). Absolute ethanol was prepared by refluxing 95% ethanol over magnesium turnings and iodine for 24 h followed by distillation. Benzene-d_6 and deuteriochloroform were used as received from MSD Isotopes. *N*-Phenylmaleimide (Sigma) was recrystallized twice from acetone and dried over phosphorus pentoxide (mp 89.5–90°C). 4-Aminobiphenyl, maleic anhydride, and *para*-terphenyl were used as received from Aldrich Chemical Co.

7-Dehydrocholesteryl acetate (**1**) was prepared from 7-dehydrocholesterol (Sigma) and acetic anhydride by the method of Prichard (36). The product was recrystallized thrice from acetone and washed with cold methanol (mp 125–127°C; lit. (37) mp 129–130°C).

N-Biphenylmaleimide (**7**) was prepared by the method of Crivello (18). The crude product was purified by column chromatography (silica; 2% acetonitrile – methylene chloride) followed by two recrystallizations from acetone, and obtained as bright yellow needles (mp 190.0–190.5°C; lit. (18) mp 189–190°C).

N-Terphenylmaleimide (**8**) was prepared by a modification of the procedure employed for the synthesis of **7** (18). Maleic anhydride (0.3 g, 3.1 mmol) was dissolved in acetone (4 mL) and 4-amino-*p*-terphenyl (38) (0.5 g, 2.04 mmol) was added, resulting in the immediate formation of a yellowish precipitate. The precipitate was collected by vacuum filtration, dried over phosphorus pentoxide in a vacuum desiccator for several hours, and then dissolved in a solution of acetic anhydride (5 mL) and anhydrous sodium acetate (0.1 g). The mixture was heated for 4 h at 90°C, during which time a yellow precipitate was formed. The mixture was cooled and the resulting solid collected and washed with acetone–water. Two recrystallizations from acetone yielded **8** as a pale yellow solid (0.55 g, 1.7 mmol, 83%); mp 293–303°C (dec.). IR (KBr) (cm^{-1}): 3095 (w), 1705 (s), 1503 (w), 1481 (m), 1394 (m), 1153 (w), 1139 (w), 1009 (w), 939 (w), 822 (m), 812 (m), 757 (w), 751 (w), 718 (w), 676 (m); ^1H NMR (200 MHz; $CDCl_3$) δ: 6.88 (s, 2H), 7.46 (m, 4H), 7.68 (s, 5H), 7.69 (m, 4H); ^{13}C NMR ($CDCl_3$) δ: 126.28, 127.02, 127.52, 127.74, 128.80, 130.29, 134.26, 139.00, 140.48, 169.50; MS *m/e*(*I*): 69(13), 169(9), 255(10), 271(11), 325(100), 326(6). Exact Mass calcd. for $C_{22}H_{15}NO_2$: 325.1103; found: 325.1105.

*Preparation and isolation of adducts from reaction of **1** and **6–8***

Preparative-scale thermolyses of **1** with **6** and **7** were carried out in the following fashion. 7-Dehydrocholesteryl acetate (**1**; 0.30 g, 0.7 mmol) and an equimolar amount of **6** or **7** were dissolved in benzene (35 mL). The resulting solution was divided among three 5/8-in. thick-walled Pyrex tubes which had been soaked in 10% aqueous sodium hydroxide for ca. 8 h, rinsed several times with distilled water, and oven-dried. The samples were degassed using three freeze–pump–thaw cycles, and the tubes were sealed under vacuum. They were then placed in a Parr model 4914 Pressure Reaction Apparatus and heated at 200°C for 4 h. The tubes were opened and the solvent was removed on the rotary evaporator.

Preparative-scale thermolysis of **1** and **8** was carried out using cholesteryl 4-chlorobenzoate (a cholesteric liquid crystal at 200°C) as solvent, in order to obtain a higher yield of adduct **10** than is afforded from the reaction in benzene solution (17). The diene **1** (0.15 g, 0.35 mmol), **8** (0.113 g, 0.35 mmol), and cholesteryl 4-chlorobenzoate (15 g) were dissolved in methylene chloride (15 mL). The volatile solvent was removed on the rotary evaporator, and the solid mixture which remained was placed in a 5/8-in. Pyrex tube, sealed under vacuum, and heated at 200°C for 4 h. The resulting mixture was flash-chromatographed on a silica gel column. The liquid crystal was eluted with 3:2 dichloromethane:hexanes, while the products were subsequently eluted as a mixture with starting materials with 2% acetonitrile in dichloromethane.

Isolation of the products from the thermolyses described above was carried out by cyclic semi-preparative liquid chromatography, using flow rates of 8–10 mL/min. The crude reaction mixtures were placed on the column. Three chromatographic cycles with methylene chloride as eluant separated the mixture into three fractions, which were collected and stripped of solvent. The first fraction, which consisted of the starting materials, was discarded. The second fraction consisted of a mixture of **9*a*** and **10**, while the third consisted of a mixture of **9*b***, **11**, and small quantities of a fifth (unidentified) adduct. Adducts **9*a*** and **10** were separated after three further cycles of the second fraction on the same column using methylene chloride as eluant. For the reaction with **6**, adducts **9*b*** and **11** were separated from the third fraction after two further cycles on the same column using 2% acetonitrile in dichloromethane as eluant. For the reaction with **7** and **8**, adducts **9*b*** and **11** were isolated by reverse-phase chromatography using 5% water in acetonitrile as eluant (7 mL/min) and a single pass through the column. The solvents were stripped from the purified adducts, and they were then recrystallized several times from methanol or chloroform–methanol mixtures. Analytical, physical, and spectroscopic data for each of the adducts are described below.

Product yields for the reaction of **1** with **6–8** in benzene solution were determined by HPLC analysis of small-scale (ca. 0.01 mmol) mixtures, which were thermolysed in base-washed, sealed 7-mm Pyrex tubes for 4 h in an oil bath at 200°C. After cooling to room temperature, the tubes were opened and aliquots were injected into the HPLC.

*Thermolysis of **1** and **6***

The adducts were separated on silica using 2% acetonitrile–dichloromethane as eluant and a flow rate of 1 mL/min. Under these conditions, the starting materials and products elute as follows: **1** (4 min); **6** (6 min); **9*a*** (13 min; 36%); **10** (14 min; 13%); **9*b*** (19 min; 25%); **11** (23.5 min; 19%); unidentified adduct (27 min; 6%).

The aryl regions in the ^1H and ^{13}C NMR spectra of the adducts were essentially identical (see **9*a*** (Ar = phenyl)).

9*a* *(Ar = phenyl):* mp 124–126°C; IR (cm^{-1}): 2959 (s,br), 2979 (m), 1715 (s), 1500 (m), 1467 (m), 1459 (m), 1385 (s), 1244 (s,br), 1215 (w), 1179 (s, br), 1034 (s), 949 (w), 931 (w), 799 (w), 755 (w), 742 (w), 693 (w); MS m/e(*I*): 599(0.5), 524(1), 424(3), 365(100), 349(15), 251(30), 197(18), 157(16). Exact Mass calcd. for $C_{39}H_{53}NO_4$: 599.3975; found: 599.3961. See Tables 1–3 for ^1H and ^{13}C NMR data for this compound.

9*b* *(Ar = phenyl):* mp 78.5–81.0°C; IR (cm^{-1}): 2960 (s, br), 2878 (m), 1719 (s,br), 1501 (m), 1468 (w), 1458 (w), 1378 (s), 1369 (s), 1260 (s), 1244 (s,br), 1174 (s, br), 1028 (s, br), 952 (w), 938 (w), 799 (m), 756 (w), 738 (w), 694 (w); ^1H NMR ($CDCl_3$): essentially identical to that of **9*b*** (Ar = biphenyl; *vide infra*), except in aryl region; ^{13}C NMR ($CDCl_3$): essentially identical to that of **9*b*** (Ar = biphenyl; *vide infra*), except in aryl region; MS *m/e*(*I*): 599(0.5), 524(2), 424(2), 365(100), 349(7), 251(10), 197(8), 157(7), 119(7). Exact Mass calcd. for $C_{39}H_{53}NO_4$: 599.3975; found: 599.3970.

10 *(Ar = phenyl):* mp 170.0–172.5°C; IR (cm^{-1}): 2957 (s, br), 2876 (m), 1714 (s,br), 1499 (m), 1467 (w), 1455 (w), 1395 (s), 1378 (m), 1359 (m), 1234 (s, br), 1209 (w), 1180 (s, br), 1158 (w), 1034 (s), 958 (w), 939 (w), 793 (m), 776 (w), 748 (w), 691 (m); MS *m/e(I)*: 599(0.8), 524(5), 424(2), 365(100), 349(5), 195(6), 157(33), 119(11), 95(10). Exact Mass calcd. for $C_{39}H_{53}NO_4$: 599.3975; found: 599.3967. See Tables 1–3 for ^1H and ^{13}C NMR data for this compound.

11 *(Ar = phenyl):* mp 96.5–98.0°C; IR (cm^{-1}): 2962 (s, br), 2879 (m), 1718 (s,br), 1500 (m), 1468 (w), 1458 (w), 1380 (s, br), 1368 (s), 1246 (s,br), 1186 (m), 1029 (m), 919 (w), 897 (w), 760 (w), 730 (w), 688 (w); MS *m/e(I)*: 599(1), 539(100), 524(20), 365(5), 351(4), 237(8), 174(50), 129(20). Exact Mass calcd. for $C_{39}H_{53}NO_4$: 599.3975; found: 599.3976. See Tables 1–3 for ^1H and ^{13}C NMR data for this compound.

Thermolysis of ***1*** *and* ***7***

The adducts were separated on silica gel using 2% acetonitrile–dichloromethane as eluant and a flow rate of 1 mL/min. Under these conditions, the starting materials and products elute as follows: **1** (4 min); **7** (5.5 min); **10** (7.5 min; 13%); ***9a*** (8.1 min; 32%); ***9b*** (11 min; 26%); and **11** (11 min; 22%); unidentified adduct (16 min; 7%).

The aryl regions in the ^1H and ^{13}C NMR spectra of the adducts were essentially identical (see ***9a*** (Ar = *para*-biphenyl)).

9a *(Ar* = para-*biphenyl):* mp 100.5–101.5°C; IR (cm^{-1}): 2956 (s,br), 2876 (m), 1714 (s, br), 1522 (m), 1485 (m), 1466 (w), 1434 (w), 1376 (s, br), 1241 (s,br), 1172 (m, br), 1027 (m,br), 833 (m), 757 (m), 692 (m), 662 (w); ^1H NMR: similar to ***9a*** (Ar = phenyl) (Fig. 1*a* and Table 1), except in aryl region; δ: 7.2–7.9 (m, 9H); ^{13}C NMR: similar to ***9a*** (Ar = phenyl) (Table 1), except in aryl region; δ: 127.2 (Bp-3′/5′), 127.8 (Bp-2′/6′), 128.2 (Bp-4′), 128.4 (Bp-3/5), 129.4 (Bp-2/6), 131.7 (Bp-1), 141.0 (Bp-1′), 142.1 (Bp-4); MS *m/e(I)*: 675(0.5), 615(2), 366(34), 365(100), 364(47), 251(25), 249(50), 237(17), 219(13), 195(32). Exact Mass calcd. for $C_{45}H_{57}NO_4$: 675.4287; found: 675.4281. Anal. calcd. for $C_{45}H_{57}NO_4$: C 79.96, H 8.50; found: C 79.44, H 8.52.

9b *(Ar* = para-*biphenyl):* mp 221.0–223.0°C; IR (cm^{-1}): 2959 (s,br), 2875 (m), 1716 (s, br), 1505 (w), 1486 (m), 1464 (w), 1444 (w), 1376 (s, br), 1243 (s,br), 1173 (m, br), 1025 (m), 817 (w), 759 (m), 690 (m), 664 (w); ^1H NMR ($CDCl_3$; assignments tentative in some cases); δ: 0.84 (d, 26), 0.85 (d, 27), 0.89 (s, 19), 0.90 (s, 18), 0.93 (d, 21), 1.03 and 1.36 (m, 22), 1.15 and 1.34 (m, 23), 1.11 (m(2H), 24), 1.15 (m, 17), 1.16 (dd, 12α), 1.24 (dd, 1α), 1.42 (m, 16α), 1.45 (m, 20), 1.51 (m, 25), 1.54 (m, 11β), 1.55 (m, 2β), 1.64 (m, 11α), 1.78 (ddd, 1β), 1.84 (m, 16α), 1.87 (m, 2α), 2.01 (dd, 12β), 2.17 (m, 15β), 2.25 (m, 9), 2.27 (m, 15α), 2.34 (m, 4β), 2.45 (ddd, 4α), 3.09 (m, 1′), 2.70 and 2.93 (dd(2H), 2′), 1.98 (s, CH_3CO), 3.16 (q, 7β), 4.61 (m, 3α), 5.51 (dd, 6), 7.2–7.9 (m, 9H); ^{13}C NMR ($CDCl_3$; assignments tentative in some cases); δ: 18.2 (18), 19.7 (11), 19.8 (19), 20.9 (21), 22.0 (CH_3CO), 23.1 (27), 23.4 (26), 24.6 (23), 26.7 (15), 27.3 (16), 28.3 (2), 28.6 (25), 34.4 (2′), 35.2 (20), 36.5 (22), 36.6 (1), 37.7 (12), 38.4 (4), 39.3 (10), 40.1 (24), 40.5 (7), 44.1 (13), 44.5 (9), 46.2 (1′), 58.3 (17), 73.8 (3), 122.0 (6), 125.9 (5), 127.4 (Bp-3′/5′), 127.9 (Bp-2′/6), 128.2 (Bp-4′), 128.7 (Bp-3/5), 129.4 (Bp-2/6), 131.7 (Bp-1), 141.0 (Bp-1′), 142.3 (Bp-4), 144.0 (14), 148.2 (8), 170.9 (CH_3CO), 176.2 (CO), 178.9 (CO); MS *m/e(I)*: 675(2), 616(14), 366(37), 365(100), 364(42), 251(22), 249(15), 237(4), 219(9) 195(19). Exact Mass calcd. for $C_{45}H_{57}NO_4$: 675.4287; found: 675.4284. Anal. calcd. for $C_{45}H_{57}NO_4$: C 79.96, H 8.50; found: C 79.57, H 8.40.

10 *(Ar* = para-*biphenyl):* mp 183.5–185.0°C; IR (cm^{-1}): 2957 (s,br), 2877 (m), 1716 (s, br), 1522 (m), 1486 (m), 1466 (w), 1451 (w), 1376 (s, br), 1245 (s,br), 1172 (m, br), 1026 (m), 836 (w), 758 (m), 692 (m), 660 (w); ^1H NMR: similar to **10** (Ar = phenyl) (Fig. 1*a* and Table 1), except in aryl region; ^{13}C NMR: similar to **10** (Ar = phenyl) (Table 1), except in aryl region; MS *m/e(I)*: 675(0.2), 616(1), 615(3), 600(4), 366(35), 365(100), 364(32), 251(22), 249(24), 195(15). Exact Mass calcd. for $C_{45}H_{57}NO_4$: 675.4287; found: 675.4314. Anal. calcd. for $C_{45}H_{57}NO_4$: C 79.96, H 8.50; found: C 79.96, H 8.56.

11 *(Ar* = para-*biphenyl):* mp 120.0–122.0°C; IR (cm^{-1}): 2956 (s,br), 2875 (m), 1715 (s, br), 1520 (m), 1486 (m), 1465 (w), 1445 (w), 1377 (s, br), 1244 (s,br), 1180 (m), 1027 (m), 832 (m), 760 (m), 739(m), 694 (m), 665 (w); ^1H NMR: similar to **11** (Ar = phenyl) (Table 1), except in aryl region; ^{13}C NMR: similar to **11** (Ar = phenyl) (Table 1), except in aryl region; MS *m/e(I)*: 675(48), 367(30), 366(100), 365(26), 364(15), 351(14), 253(18), 251(11), 250(19), 249(89), 195(16). Exact Mass calcd. for $C_{45}H_{57}NO_4$: 675.4287; found: 675.4289.

Thermolysis of ***1*** *and* ***8***

The adducts were separated on silica using 2% acetonitrile–dichloromethane as eluant and a flow rate of 1 mL/min. Under these conditions, the starting materials and products elute as follows: **1** (4 min); **8** (5.0 min); **10** (6 min; 15%); ***9a*** (7 min; 32%); ***9b*** (10 min; 26%); and **11** (10 min; 21%), unidentified adduct (13 min; 7%). Thermolysis of **1** and **8** in the cholesteric liquid-crystalline phase of cholesteryl-4-chlorobenzoate for 4 h at 200°C yields the same products, but in the following yields: **10** (40%), ***9a*** (21%), ***9b*** (13%), **11** (10%), unidentified adduct (16%).

The aryl regions in the ^1H and ^{13}C NMR spectra of the adducts were essentially identical (see ***9a*** (Ar = *para,para′*-phenyl)).

9a *(Ar* = para,para′-*terphenyl):* mp 147.5–1.49.5°C; IR (cm^{-1}): 2939 (s,br), 2861 (s), 1713 (s, br), 1508 (w), 1487 (m), 1465 (m), 1380 (s, br), 1240 (s,br), 1169 (m, br), 1029 (w), 820 (w), 760 (m), 730 (w), 691 (w); ^1H NMR: similar to ***9a*** (Ar = phenyl) (Fig. 1*a* and Table 1), except in aryl region; δ: 7.2–7.9 (m, 13H); ^{13}C NMR: similar to ***9a*** (Ar = phenyl) (Table 1), except in aryl region; MS *m/e(I)*: 751(1), 424(2), 367(6), 366(32), 365(100), 364(47), 325(21), 271(14), 157(10). Exact Mass calcd. for $C_{51}H_{64}NO_4$: 751.4601; found: 751.4579.

9b *(Ar* = para,para′-*terphenyl):* mp 182.0–185.0°C; IR (cm^{-1}): 2942 (s,br), 2862 (m), 1715 (s, br), 1478 (m), 1459 (w), 1370 (s, br), 1230 (m,br), 1167 (m, br), 1020 (m, br), 683 (w); ^1H NMR ($CDCl_3$): essentially identical to that of ***9b*** (Ar = biphenyl; *vide supra*), except in aryl region; ^{13}C NMR ($CDCl_3$): essentially identical to that of ***9b*** (Ar = biphenyl; *vide supra*), except in aryl region; MS *m/e(I)*: 751(1), 424(2), 367(8), 366(38), 365(100), 364(52), 325(34), 271(18). Exact Mass calcd. for $C_{51}H_{64}NO_4$: 751.4601; found: 751.4579.

10 *(Ar* = para,para′-*terphenyl):* mp 162–166°C; IR (cm^{-1}): 2937 (s,br), 2860 (m), 1715 (s, br), 1510 (m), 1485 (w), 1466 (m), 1384 (s), 1240 (s,br), 1166 (m, br), 1032 (m), 824 (m), 760 (m), 730 (w), 692 (w); ^1H NMR: similar to **10** (Ar = phenyl) (Fig. 1*a* and Table 1), except in aryl region; ^{13}C NMR: similar to **10** (Ar = phenyl) (Table 1), except in aryl region; MS *m/e(I)*: 751(0.5), 424(2), 367(7), 366(33), 365(100), 364(38), 325(21), 271(12), 213(17), 157(31). Exact Mass calcd. for $C_{51}H_{64}NO_4$: 751.4601; found: 751.4579.

11 *(Ar* = para,para′-*terphenyl):* mp 119.5–123.0°C; IR (cm^{-1}): 2959 (s,br), 2878 (s), 1715 (s, br), 1508 (w), 1485 (m), 1467 (m, br), 1379 (s, br), 1244 (s,br), 1179 (m, br), 1028 (w), 820 (m), 762 (m), 745 (w), 732 (w), 691 (m); ^1H NMR: similar to **11** (Ar = phenyl) (Table 1), except in aryl region; ^{13}C NMR: similar to **11** (Ar = phenyl) (Table 1), except in aryl region; MS *m/e(I)*: 751(77), 366(100), 325(82), 271(20), 195(12). Exact Mass calcd. for $C_{51}H_{64}NO_4$: 751.4601; found: 751.4606.

Acknowledgements

We wish to thank the McMaster University Regional Centre for Mass Spectrometry for the mass spectrometric analyses, and the Natural Sciences and Engineering Research Council of Canada for its generous financial support.

1. A. Van der Gen, J. Lakeman, M. A. M. P. Gras, and H. O. Huisman. Tetrahedron, **20**, 2521 (1964).
2. M. Anastasia, A. Fiecchi, and G. Galli. J. Org. Chem. **46**, 3421 (1981).
3. J. Lakeman, W. N. Speckamp, and H. O. Huisman. Tetrahedron, **24**, 5151 (1968).
4. A. Van der Gen, J. Lakeman, U. K. Pandit, and H. O. Huisman. Tetrahedron, **21**, 3641 (1965).
5. F. Snatzke and H. P. Wolff. Liebigs Ann. Chem. 468 (1985).
6. D. N. Jones, P. F. Greenhalgh, and I. Thomas. Tetrahedron, **24**, 5215 (1968).
7. D. H. R. Barton, T. Shioiri, and D. A. Widdowson. J. Chem. Soc. C, 1968 (1971).
8. M. Tada and A. Oikawa. J. Chem. Soc. Perkin Trans. 1, 1858 (1979).
9. M. K. Shakhova, V. A. Kostoglodova, and G. I. Samokhvalov. J. Gen. Chem. USSR, **46**, 1598 (1976).
10. D. H. R. Barton, G. LeClerc, P. D. Magnus, and I. D. Menzies. J. Chem. Soc. Chem. Commun. 447 (1972).
11. A. Van der Gen, W. A. Zunnebald, U. K. Pandit, and H. O. Huisman. Tetrahedron, **21**, 3651 (1965).
12. A. Windaus and A. Luttringhaus. Ber. Dtsch. Chem. Ges. **64**, 850 (1931).
13. (*a*) H. H. Inhoffen. Justus Liebigs Ann. Chem. **508**, 81 (1934); (*b*) E. M. Hicks, C. J. Berg, and E. S. Wallis. J. Biol. Chem. **162**, 654 (1946); (*c*) K. Schubert and K.-H. Bohme. Chem. Ber. **93**, 1878 (1960); (*d*) D. N. Jones and I. Thomas. J. Chem. Soc. 5206 (1964).
14. D. N. Jones, P. F. Greenhalgh, and I. Thomas. Tetrahedron, **24**, 297 (1968).
15. W. J. Leigh. *In* Liquid crystals. Applications and uses. Vol. II. *Edited by* B. Bahadur. World Scientific, Singapore. 1990; and references cited therein.
16. W. J. Leigh and D. S. Mitchell. J. Am. Chem. Soc. **110**, 1311 (1988).
17. W. J. Leigh and D. S. Mitchell. J. Am. Chem. Soc. **114**, 5005 (1992).
18. J. V. Crivello. J. Polymer Sci. Polymer Chem. Ed. **14**, 159 (1976).
19. (*a*) R. R. Ernst, G. Bodenhausen, and A. Wokaun. Principles of nuclear magnetic resonance in one and two dimensions. Oxford Science Publications, Oxford. 1987; (*b*) J. K. M. Sanders and B. K. Hunter. Modern NMR spectroscopy — A guide for chemists. Oxford University Press, Oxford. 1987.
20. (*a*) W. B. Smith. Org. Magn. Reson. **9**, 644 (1977); (*b*) R. E. Perrier and M. J. McGlinchey. Can. J. Chem. **66**, 3003 (1988).
21. D. N. Kirk, H. C. Toms, C. Douglas, K. A. White, K. E. Smith, S. Latif, and R. W. P. Hubbard. J. Chem. Soc. Perkin Trans. 2, 1567 (1990).
22. J. Drew, J.-R. Brisson, P. Morand, and A. G. Szabo. Can. J. Chem. **65**, 1784 (1987).
23. J. B. Stothers. Carbon-13 NMR spectroscopy. Academic Press, New York. 1972. pp. 439–443.
24. L. M. Jackman and S. Sternhell. Applications of nuclear magnetic resonance spectroscopy in organic chemistry. 2nd ed. Pergamon Press, Oxford. 1969. p. 325.
25. H. Booth. Prog. NMR Spectrosc. **5**, 149 (1969).
26. M. Barfield and D. M. Grant. J. Am. Chem. Soc. **85**, 1899 (1963).
27. A. A. Bothner-By. Advances in magnetic resonance. Vol. I. *Edited by* J. S. Waugh. Academic Press, New York. 1965. p. 195.
28. (*a*) L. Braunschweiler and R. R. Ernst. J. Magn. Reson. **53**, 521 (1983); (*b*) A. Bax and D. G. Davies. J. Magn. Reson. **65**, 355 (1985).
29. D. Marion and K. Wuthrich. Biochem. Biophys. Res. Commun. **113**, 967 (1983).
30. G. Bodenhausen, H. Kogler, and R. R. Ernst. J. Magn. Reson. **58**, 370 (1984).
31. A. Bax. J. Magn. Reson. **53**, 517 (1983).
32. V. Rutar. J. Magn. Reson. **58**, 306 (1984).
33. J. A. Wilde and P. H. Bolton. J. Magn. Reson. **59**, 343 (1985).
34. A. Bax and S. Subramanian. J. Magn. Reson. **67**, 565 (1986).
35. A. J. Shaka, P. B. Barker, and R. Freeman. J. Magn. Reson. **64**, 547 (1985).
36. W. W. Prichard. Org. Synth. **28**, 68 (1948).
37. H. Schaltegger. Helv. Chim. Acta, **33**, 2101 (1950).
38. R. G. Splies. J. Org. Chem. **26**, 2601 (1961).
39. R. W. Kriwacki and T. P. Pitner. Pharm. Res. **6**, 531 (1989).
40. D. Neuhaus and M. P. Williamson. *In* The nuclear Overhauser effect in structural and conformational analysis. VCH Publishers, New York. 1989.